A.H. Fadhil
Materials Engineering Department- University of Technology, Iraq
hashembsb@yahoo.com

S. A. Emad
Materials Engineering Department- University of Technology, Iraq

K.H. Abbas
Materials Engineering Department- University of Technology, Iraq

H. A. Olaa
Materials Engineering Department- University of Technology, Iraq

Received on: 28/09/2016
Accepted on: 29/12/2016

Welding procedures of Turbine Blades by Using ER 309L Austenitic Filler Wire

Abstract-*In the present work it has been investigated the repair of LP-blades steam turbine made of AISI 410 martensitic stainless steels (MSS) by GTAW welding, the repair welding carried out by using ER 309L as consumable filler wire. PWHT was carried out at 1100°C for 1h. The structure-property relationships of the weldments were established based on the current modes employed by utilizing combined techniques of optical microscopy, line/point and EDS analysis. Results showed that Micro-hardness along the base and HAZ regions increased after PWHT as compared to in state of as-welded. After welding process, microstructure photographs of weld-metal region revealed two phase the vermicular δ-Ferrite and γ-austenite matrix. HAZ region consisted of tempered lath martensite with carbides. Line/Point analysis revealed the direction of segregation, whereas chromium was increased in core and depleted in boundary, while nickel was depleted in core and increased in boundary, this support the δ – ferrite was primarily solidified.*

Keywords- *Steam Turbine, LP- blades, GTRW, Repair welding, PWHT, martensitic stainless steels (MSS).*

How to cite this article: A.H. Fadhil, S.A. Emad, K.H. Abbas and H.A. Olaa, "Welding procedures of Turbine Blades by Using ER 309L Austenitic Filler Wire," *Engineering and Technology Journal*, Vol. ٣٥, Part A, No. ١, pp. 68-75, 2017.

1. Introduction

Gas and steam power plants in Iraq appeared to be off important options of the electrical energy. These plants contain of several number of units and components that must be work together in proper way to achieve the best efficiency and performance. In worldwide, Steam turbines considered mainstay production of electricity worldwide, since nearly 80% of the whole generated electricity by the use of steam turbines. Today's the competition in the market of electricity generation market has been increased the pressure to keep planet generation of power on line whenever required maintenance of steam turbine is of quite importance to insurance the high steam turbines efficiency and to keep safety standards in order to avoid any unexpected dangers. The steam turbines operate under high steam pressure, and have parts that require extremely high velocities. Turbine nozzles and blades are designed via accurate analysis and manufactured with high degree of finishing and accuracy Patil [1]. Bhaduri [2] investigated the developed of welding repair procedure on cracked blades steam turbine was made from MSS (martensitic stainless steel) by using TIG (Tungsten Inert Gas) welding process with consumable filler wire as ER 410 MSS and ER 316L austenitic filler wires. Results showed that employing ER 410 filler wire with preheating and PWHT processes is appropriate to weld MSS blades turbine. Divya [3] investigated the details in-situ weld repair of cracked shrouds of turbine and characterization the weld joint. Crack shrouds of the 3rd stage of a Low Pressure turbine was in-situ repaired by removing the cracked pieces of the shroud that made of AISI 414 martensitic stainless steel (SS) and welding using gas tungsten arc welding with ER 410NiMo consumable wire. Micro-hardness result showed weld-metal region in state as welded and after heat treated was reduced from 400-260 VHN with applied load 500g. Sara [4], studied the metallurgical transformations accruing through SMAW welding of AISI 316L austenitic stainless steel with AISI 430 ferritic stainless steel. AWS E309L austenitic and AWS E2209-16 duplex stainless steels were using as filler wires to perform this study. Microstructural results of a dissimilar austenite- ferrite stainless steel welding using two different filler metals was showed, the morphology and amount of delta ferrite is a function of the chemical composition of the filler

https://doi.org/10.30684/etj.2017.127312
412-0758/University of Technology-Iraq, Baghdad, Iraq2

metal. Arivarasu [5] investigated dissimilar welding joint between AISI 304L (ASS) and low alloyed AISI 4340 aeronautical steel that welded joint by CC (continuous current) and PC (pulsed current) GTAW techniques, using two types of consumables filler metal as ER309L and ERNiCr-3. optical microstructure results of the weldments joined by CCGTAW with 2 consumable filler metals was showed weld-metal was revealed coarser microstructure contained columnar dendrites with appearances of secondary phase (s) at the interface of AISI 4340 side. The aim of the present research is investigation the developed repair welding procedure to repair turbine blades with using ER 309L austenitic filler wire. Also, the effects of post-weld treatments were studied on the microstructural, hardness and chemical composition of the welded joints of AISI 410MSS/ER309L.

2- Materials and Experimental Procedure

LP blades of a steam turbine made from AISI 410 martensitic stainless steel used as a base metal. ER 309L austenitic filler metal is candidate and employed, chemical composition for 410MSS and ER309L is represented in Table 1.

The blades were sectioned by the spark discharge machine (EDM) to the pair's symmetry (each piece of pair's has dimensioned approximately (25mm*100mm). Followed by, it is achieved standard V-Butt configurations (single V-groove having a root face of 2 mm, size land of 1 mm and included angle of 70°) was worked on these pair's. Multi-pass welding was performed through TIG welding machine (type/ ESAB LRT 160, Materials Engineering, University of technology)and V-butt welding joint process was depended on the skill of welder; Figure 1, illustrated specimens after welding. No preheating was made before welding to a void hydrogen induced cracks. The parameters of welding joint were fixed: - Main Supply 70-80 V/Hz, Current Range 130 A and Gas Flow Rate 6 L/min-1. When welding process was completed, the samples were cute by Wire Electrical Discharge Machining (WEM) or Wire-Cut EDM (type/ Smart DEM), to small specimens with dimension (50 * 10 * 10) mm, as shown in Figure 2. After welding and cutting process, each sectioned specimen was subjected to PWHT (Post Weld Heat Treatment) in order to obtained best mechanical properties and some stress relief. PWHT method was conducted at 1100 ^{o}C. PWHT was carried out by using furnace (type/Carbolite 1200). The holding time for PWHT was 1hr and cooling rate 30 C^{o}/min. The furnace was switched off and cross-section specimens were placed in to slowly cool to room temperature in order to prevent high-temperature oxidation of the joint.

Table 1:- Chemical Composition of Base Metal and Filler Alloys

Base/Filler metal	Chemical Composition (% by Weight)									
	C%	Cr%	Ni%	Mo%	Mn%	Si%	Fe%	Creq	Nieq	req/Nieq
AISI 410	0.127	11.94	0.2	0.0109	0.755	0.38	B	--	---	---
ER 309L	3.79	21.24	14.24	1.04	1.87	0.73	57.1	23.3	15.2	1.53

Cr eq & Ni eq estimated from Shaeffler-Delong diagram assuming N=0.03wt%.

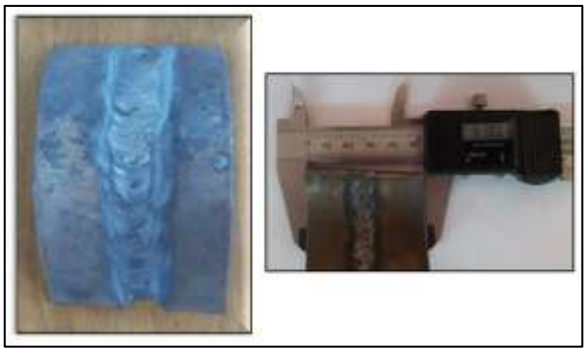

Figure 1: Specimen after welding

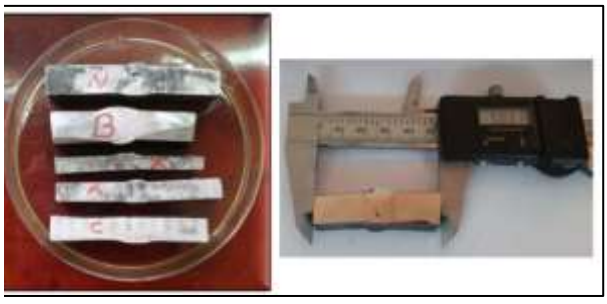

Figure 2: Specimen after cutting

I. Microstructure and Micro-hardness Testes

After grinding, polishing and etching (metallography procedure), microstructure and micro hardness along weldments studied. Optical microscope with 5 mega pixel CCD camera into image pro software with the magnification of 5, 10, and 20X used to examine samples after grinding and polishing processes.

The Vickers micro hardness test (HVS-1000) with diamond indenter was conducted on the polished mounted weld cross section, with load of 1Kg and duration time 15 seconds. Samples were prepared in accordance with to ASTM E3-11 standard [6].

II. Line/Point with EDS analysis

Electron probe micro-analyzer (EPMA), Houses a JEOL 8200 Super probe EPMA device at Microprobe Laboratory in the Department of Earth Sciences at the University of Dalhousie in Canada Country was used to complete these tests. Specimens were prepared by grinding and polishing with dimension (50 * 10 * 10) mm and then making set of points along weldments across base, HAZ and weld-metal regions, each of these points have been analyzed.

3. Results and discussion

I. Microstructure Test Results

1. Weldment AISI 410/ER 309L before PWHT

Profile concentration of ER 309 stainless steel consisted of 57.1% Fe, 21.24% Cr and 14.24% Ni by weight as mention in Table 1. Depending on Cr-Ni content 21.24/14.24, weld-metal zone consist of two phases δ - ferrite in the vermicular or skeletal form (dark etching) and austenite matrix (light etching), as shown in Figure 3. δ - Ferrite crystals firstly formed from the melt. With higher nickel content, γ crystals are also precipitated from the melt apart from crystals in the three phase (L + δ + γ) sector. After solidification completed, transformation of a ferrite into austenite (δ - γ transformation starts almost simultaneously, the structure being completely transformed into austenite with residual δ - ferrite. When Cr:Ni ratio is equal to 1.53%, the solidification mode found to be ferritic-austenitic (FA) with moderate cooling rate and the final microstructure of weld-metal zone presents vermicular δ-Ferrite as a primary phase within the dendritic arms enveloped by the austenite. Liquid-solid interface, also called solidification front, represents the boundary between melt and precipitated crystal. Weld-metal zone (fusion zone) is predominantly of columnar dendrites, which nucleated at the fusion boundary, and grown towards the center of the molten pool (opposite to the direction of heat flow). The existence of columnar dendrites structure is predominantly due to the moderate cooling rate used in the TIG welded melt pool. HAZ affected zone heated during welding to various temperatures ranging from ambient temperature to the melting range of the alloy. The grain growth occurs in the HAZ AISI 410 MSS appeared tampered lath marten site with carbides as shown in Figure 4. Whereas, with high carbon content, carbon may precipitated at HAZ region (α matrix (FCC)) in the form of carbides as M23C6 and M7C3 or M6C, due to carbon solubility at ambient temperature became very low about 0.006% in austenitic steels and even lower in ferritic steels, as reported by Erich Folkhard [7].

2. Weldment AISI 410/ER 309L after 1100°C/1h

Figure 5, showed the presence of fully austenite (light etching) of ER 309 weld-metal zone after heat treated 1100°C/1h, this may belong to the dissolution of all phases residual δ-ferrite phase and carbides at 1100°C and homogenous weld-metal zone structure formed. According to Erich Folkhard [7], austenitic steels always preferred subjected to a solution annealing treatment between 1050-1100°C at which phases including carbide M23C6, sigma phase and delta ferrite were completely dissolved and the annealing process produces a homogenous fully austenitic structure.

Figure 6, illustrated liquid-solid interface and HAZ regions. Liquid-solid interface appeared as sharp line between weld-metal zone and HAZ. Also, HAZ region has tempered lath marten site structure which was consisted of α-Ferrite (BCC) and carbides.

III. Line/Point and EDS Analysis Results

1. Weldment AISI 410/ER 309L before PWHT

Line/point analysis and EDS results showed the chemical composition of weld-metal region, as shown in Figure 7. These results showed presence of Mo in weld-metal zone center. Average Mo was found equal 1.48% along weld-metal zone center, Mo element was constricted area of γ phase, while its supported δ – ferrite formation. Also it observed from Figures 7 (A and B), that the line/point analysis was austenite at center of weld metal zone at point (Pt1) enricher by nickel, at which Cr and Ni content were found 19.19% and 11.90% respectively. While at point (Pt2) the analysis appeared residual delta ferrite and the content of Cr and Ni elements were 20.22% and 9.67% respectively. In electric arc welding, δ - γ transformation is normally passed through rather quickly and an impeded equalization of alloy concentration is to be expected. Impediment is

greater on the side of precipitated austenite crystals than on the ferrite. Moreover, it can be noted from Figure (7) and (8), line/point analysis of weld-metal zone and initial weld boundary that at point (Pt1) in Figure 8 (A and B)

Figure 3: Weld-Metal Microstructure in st

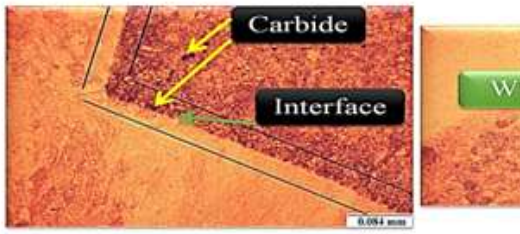

Figure 4:- Solid-Liquid Interface and HAZ Zone of 410

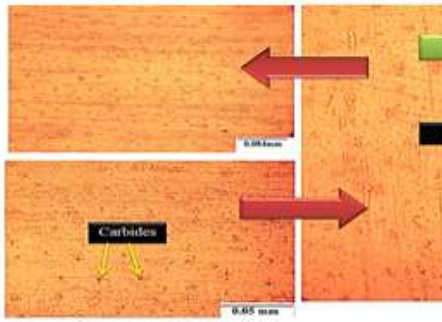

Figure 5: Weld-Metal Zone for AISI 410 MSS/ ER 309

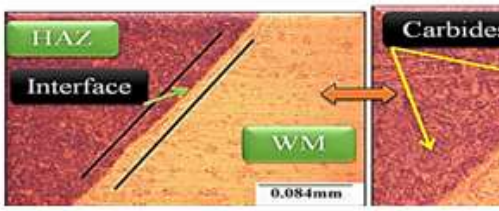

Figure 6:- A) Liquid-Solid Interface with HAZ Affected Z
after PWHT 1100□C/1h

Chromium and Nickel contents were 20.04% and 4.63% respectively. While in Figure 7 (A and B) at point (Pt1) at weld-metal zone, chromium and Nickel contents were 19.19% and 11.90% respectively. This was agreed with Erich Folkhard [7], the author has reported when solidification is mainly δ - ferrite, the segregation of chromium was increased in core and depleted in boundary, while nickel was depleted in core and increased in boundary, this means δ – ferrite was primarily solidified.

Line/point analysis at HAZ showed; the presence of Fe, Cr and C elements richly along HAZ, as shown in Figure 9. Average C content along HAZ was 2.5%. Excess carbon may precipitate in the form of chromium-iron carbides, mainly as M23C6, and in rarely as M7C3 or M6C. M23C6 were agglomerated at liquid-solid interface and precipitated as coarse or finer particles at the grain boundaries and within the grain areas.

2. Weldment AISI 410/ER 309L after 1100°C/1h

Line/point analysis and EDS analysis results showed the chemical composition of weld-metal zone after heat treated, as shown in Figure 10. As can be noticed from Figure 10 (A and B) the presence of Cr and Ni content along weld-metal zone center at which Cr content were18.26%, 19.69%, 19.33%, 17.84%, 18.29% and 19.34%. Also, Ni content were equal to12.83%, 8.76%, 10.58%, 11.81%, 10.87% and 9.73%, this supported the existence of austenite phase in all weld-metal rejoin. In addition, the analysis appeared presence of C and Mn in average 1.3% and 1.3% respectively along weld zone, because during heat treatment carbon has more activity to diffuse from carbides at HAZ regions and then cross interface toward weld-metal zone as compared weld-metal zone in state as-welded.

These elements C, Ni and Mn act as stabilizer to austenite phase. Also, the presence of molybdenum was of importance for this heat treatment, since C and Mo elements shift the boundary of the γ range to higher temperatures. Microstructure photographs of weld-metal shown in Figure 5 revealed the presences of carbides in weld-metal zone. Also, X-Ray analysis with magnification 250µm shown in Figure 10 approved the presence of these carbides as black points, because as the temperature drops down to ambient temperature the solubility of carbon reduced and tend to precipitate as carbides.

Figure 11, illustrated Line/point analysis with EDS analysis along HAZ region. This analysis resulted the presences of Fe, Cr, C, Si, Mn, Al, V and Ni along HAZ region. And the average content of C was 2.47 % along HAZ rejoin, which was precipitated as carbides with Cr or Fe or mixed carbides as former (FeCr)23C6. Chemical composition of HAZ after 1100°C/1h was similar to chemical composition for HAZ in state as-welded.

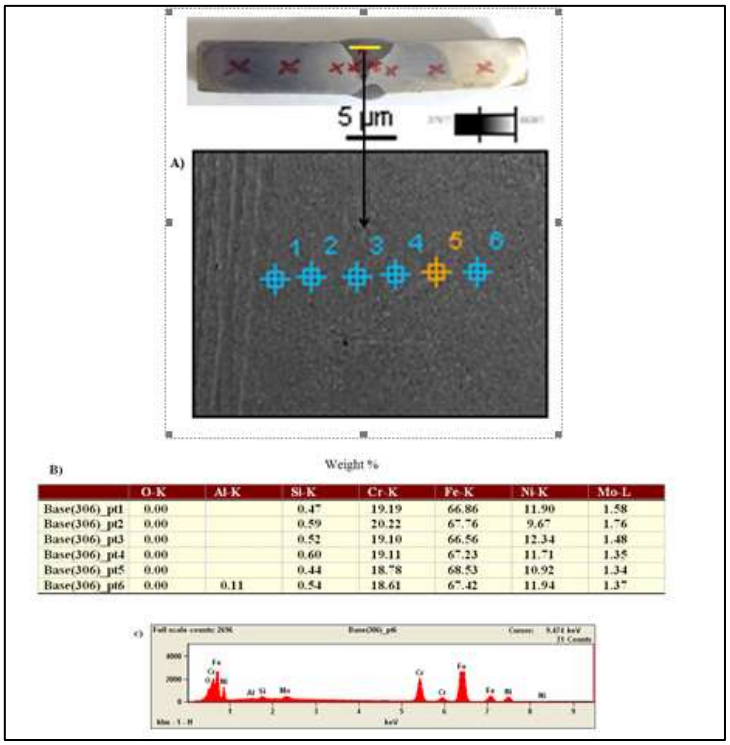

	O-K	Al-K	Si-K	Cr-K	Fe-K	Ni-K	Mo-L
Base(306)_pt1	0.00		0.47	19.19	66.86	11.90	1.58
Base(306)_pt2	0.00		0.59	20.22	67.76	9.67	1.76
Base(306)_pt3	0.00		0.52	19.10	66.56	12.34	1.48
Base(306)_pt4	0.00		0.60	19.11	67.23	11.71	1.35
Base(306)_pt5	0.00		0.44	18.78	68.53	10.92	1.34
Base(306)_pt6	0.00	0.11	0.54	18.61	67.42	11.94	1.37

Figure 7: A) Line Analysis B) Point Analysis C) EDS Analysis at Weld-Metal Zone for Weldment AISI 410MSS/ ER 309L (As-Welded)

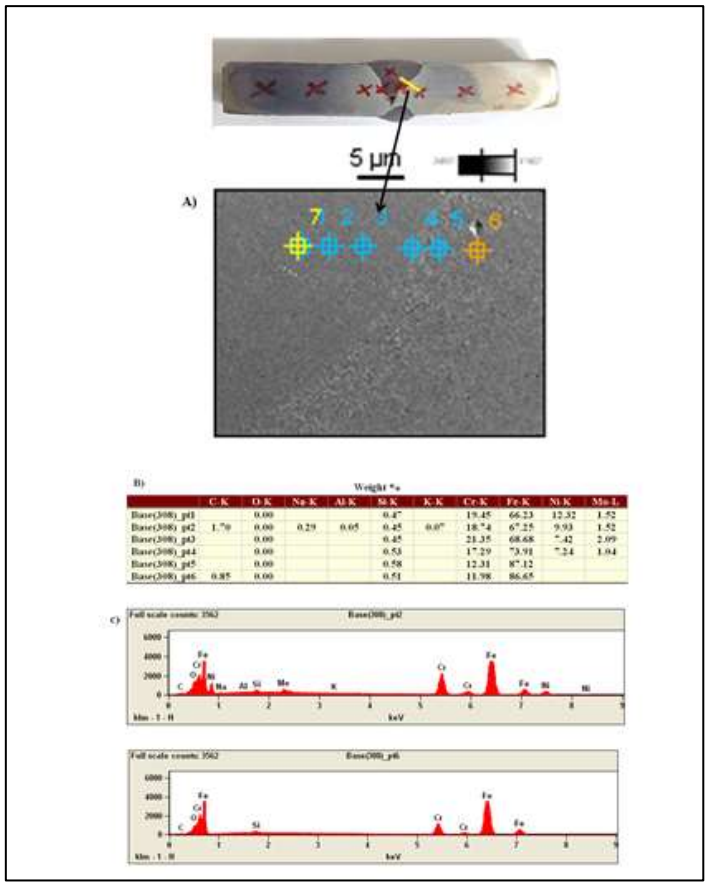

Figure 8:- A) Line Analysis B) Point Analysis C) EDS Analysis at Interface for Weldment AISI 410MSS/ ER 309L (As-Welded)

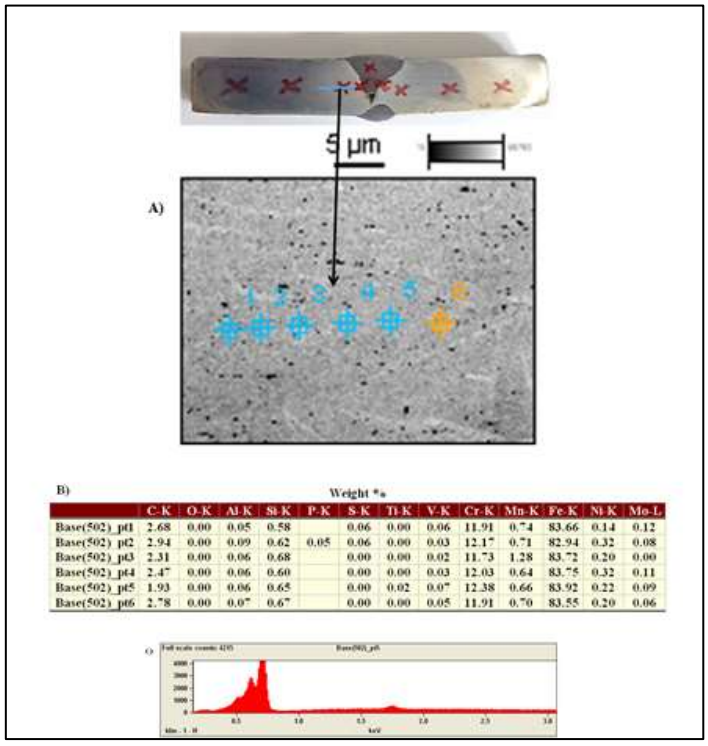

	C-K	O-K	Al-K	Si-K	P-K	S-K	Ti-K	V-K	Cr-K	Mn-K	Fe-K	Ni-K	Mo-L
Base(502)_pt1	2.68	0.00	0.05	0.58		0.06	0.00	0.06	11.91	0.74	83.66	0.14	0.12
Base(502)_pt2	2.94	0.00	0.09	0.62	0.05	0.06	0.00	0.03	12.17	0.71	82.94	0.32	0.08
Base(502)_pt3	2.31	0.00	0.06	0.68		0.00	0.00	0.02	11.73	1.28	83.72	0.20	0.00
Base(502)_pt4	2.47	0.00	0.06	0.60		0.00	0.00	0.03	12.03	0.64	83.75	0.32	0.11
Base(502)_pt5	1.93	0.00	0.06	0.65		0.00	0.02	0.07	12.38	0.66	83.92	0.22	0.09
Base(502)_pt6	2.78	0.00	0.07	0.67		0.00	0.00	0.05	11.91	0.70	83.55	0.20	0.06

Figure 9: A) Line Analysis B) Point Analysis C) EDS Analysis at HAZ Region for Weldment AISI 410MSS/ ER 309L (As-Welded)

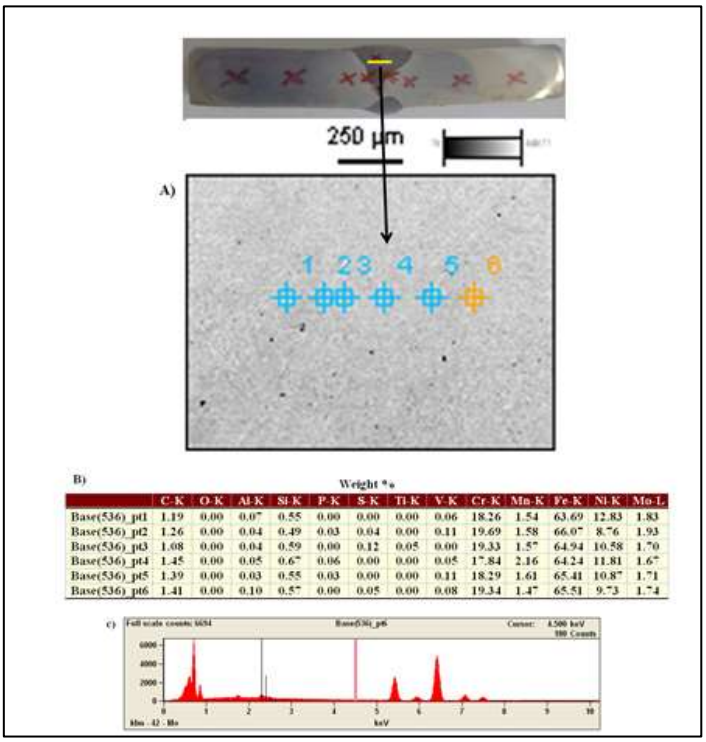

	C-K	O-K	Al-K	Si-K	P-K	S-K	Ti-K	V-K	Cr-K	Mn-K	Fe-K	Ni-K	Mo-L
Base(536)_pt1	1.19	0.00	0.07	0.55	0.00	0.00	0.00	0.06	18.26	1.54	63.69	12.83	1.83
Base(536)_pt2	1.26	0.00	0.04	0.49	0.03	0.04	0.00	0.11	19.69	1.58	66.07	8.76	1.93
Base(536)_pt3	1.08	0.00	0.04	0.59	0.00	0.12	0.05	0.00	19.33	1.57	64.94	10.58	1.70
Base(536)_pt4	1.45	0.00	0.05	0.67	0.06	0.00	0.00	0.05	17.84	2.16	64.24	11.81	1.67
Base(536)_pt5	1.39	0.00	0.03	0.55	0.03	0.00	0.00	0.11	18.29	1.61	65.41	10.87	1.71
Base(536)_pt6	1.41	0.00	0.10	0.57	0.00	0.05	0.00	0.08	19.34	1.47	65.51	9.73	1.74

Figure 10: A) Line Analysis B) Point Analysis C) EDS Analysis at Weld-Metal Regionfor AISI 410MSS/ ER 309L after PWHT 1100°C/1h

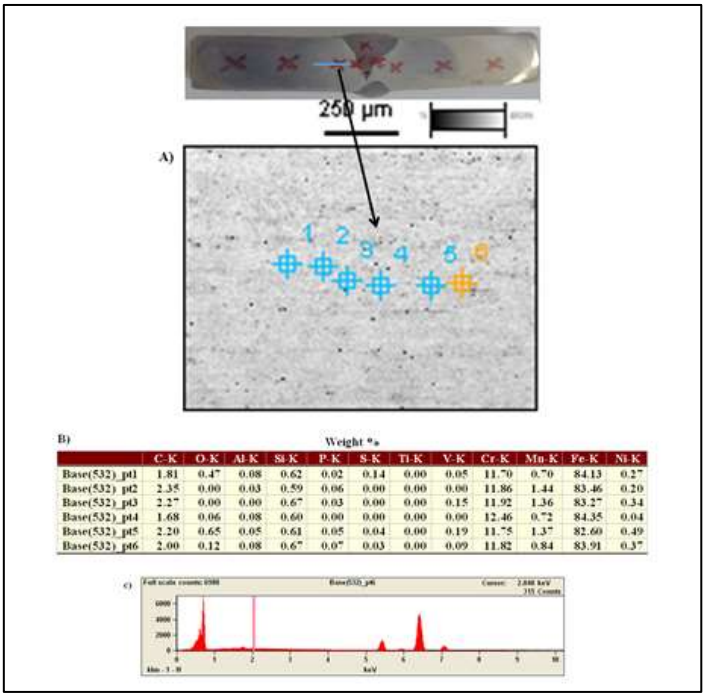

	C-K	O-K	Al-K	Si-K	P-K	S-K	Ti-K	V-K	Cr-K	Mn-K	Fe-K	Ni-K
Base(532)_pt1	1.81	0.47	0.08	0.62	0.02	0.14	0.00	0.05	11.70	0.70	84.13	0.27
Base(532)_pt2	2.35	0.00	0.03	0.59	0.06	0.00	0.00	0.00	11.86	1.44	83.46	0.20
Base(532)_pt3	2.27	0.00	0.00	0.67	0.03	0.00	0.00	0.15	11.92	1.36	83.27	0.34
Base(532)_pt4	1.68	0.06	0.08	0.60	0.00	0.00	0.00	0.00	12.46	0.72	84.35	0.04
Base(532)_pt5	2.20	0.65	0.05	0.61	0.05	0.04	0.00	0.19	11.75	1.37	82.60	0.49
Base(532)_pt6	2.00	0.12	0.08	0.67	0.07	0.03	0.00	0.09	11.82	0.84	83.91	0.37

Figure 11: A) Line Analysis B) Point Analysis C) EDS Analysis at HAZ Regions Weldment AISI 410MSS/ ER 309L after PWHT 1100°C/1h

IV. Micro-hardness Test Results

Typical micro-hardness profiles across weldment 410 MSS/ ER 309L before PWHT (as-welded) and after PWHT 1100°C/1h were showed in Figure 12. Results showed variation in micro hardness profile before and after the heat treatment depending on dilution from the base metal and weld-metal zone. Moreover, the average hardness of the HAZ and base regions was increased from HV 416.9, 251.3 in state as-welded to HV 449, 426.3 after PWHT 1100°C/1h respectively. Finally, hardness results showed increment along HAZ region in state as welded due to carbon aggregated at interface and increased again after heat treatment due to more carbides formed above 500°C.

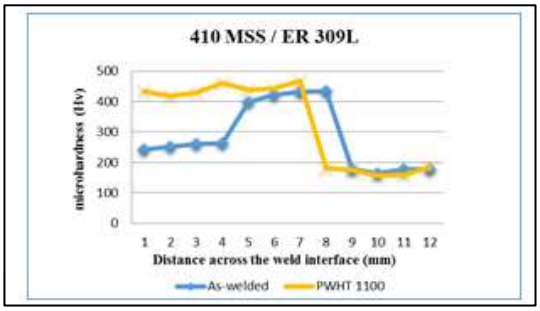

Figure12: Micro-hardness Variation across the 410 MSS/ ER 309L before PWHT (as-welded) and after PWHT 1100°C/1h

4. Conclusions

The present study has investigated the repair of turbine blades by using ER309L as austenitic filler metals and studied the effect PWHT on structure and properties of weldments:

- After welding process, weld-metal region consisted of two phases δ - ferrite in the skeletal form and austenite matrix, while after heat treated weld-metal region consisted of homogenous austenite phase.
- C, Mn, Ti, V and Al elements moved toward weld-metal region after heat treatment.
- Large amounts from carbon elements aggregated at HAZ region close to interface in state as-welded and after 1100°C/1h.
- Average hardness at the weld-metal zone was increased from HV 172.2 to 176.1, also, the hardness of the alloy increased after heat treated along base and HAZ regions.
- Segregation of elements was reduced after 1100°C/1h.

5. Acknowledgement

This work didn't fund by any government institution.

References

[1] H.G. Patil and V.G. Arajpure, "Improvements to opening and closing appraisal method of low pressure steam turbine performance predication," International Journal of Research in Aeronautical and Mechanical Engineering, Vol. 2, No. 2, 43-55, 2014.

[2] A.K. Bhaduri, T.P.S. Gill, S.K. Albert, K. Shanmugam and D.R. Iyer, "Repair welding of cracked steam turbine blades using austenitic and martensitic stainless-steel consumables," Nuclear Engineering and Design, Vol. 34, No. 23, 249-259, 2001.

[3] M. Divya, C.R. Das, S.K. Albert, V. Ramasubbu, A.K. Bhaduri and P. Sivaraman., "In-situ weld repair of cracked shrouds of turbine and characterization of the weld joint," Ommi, 1-11, 2011.

[4] A. Sara, T. Ramón, S. Claudia,"Microstructural transformations of dissimilar austenite-ferrite stainless steels welded joints", Journal of Materials Physics and Chemistry, Vol. 1, Issue. 4, 65-68, 2013.

[5] M. Arivarasua, D.R. Kasinatha, A. Natarajan, "Effect of continuous and pulsed current on the metallurgical and mechanical properties of gas tungsten arc welded aisi 4340 aeronautical and aisi 304 l austenitic stainless steel dissimilar joints," Materials Research, Vol. 18, 59-77, 2015.

[6] E3-11 "Standard guide for preparation of metallographic specimens, alloys, specimens," ASTM International, West Conshohocken, PA, 2011.

[7] E. Folkhard, "Welding metallurgy of stainless steels,"", Springer-Verlag/Wien," New York, ISBN-13978-3-7091-8967-2, 1988.

Author's biography

Assist. Prof. A.H. Fadhil is with metal engineering, Department of Materials Engineering, University of Technology, Iraq. He has been working on various aspects related to welding of materials. His areas of interest include repair welding, dissimilar metal joining, development of hard facing technology.

Assist. Prof. S.A. Emad is with metal engineering, Materials Engineering Department, University of Technology, Iraq. He has been working on various aspects related to shape memory alloys and biomedical metals.

Assist. Prof. Abbas K. Husain is with metal engineering, Materials Engineering Department, University of Technology, Iraq. He has been working on various aspects related to welding, corrosion and coating of materials.

Dr. H.A. Ola is withmetal engineering, engineering, Materials Engineering Department- University of Technology, Baghdad, Iraq. She has been working on welding of materials and composite material